References

BRAGG, W. L. & HOWELLS, E. R. (1954). *Acta Cryst.* **7**, 409.

COCHRAN, W. & HOWELLS, E. R. (1954). *Acta Cryst.* **7**, 412.

FOCK, V. A. & KOLPINSKY, V. A. (1940). *J. Phys. U.S.S.R.* **3**, 125.

JAGODZINSKI, H. & KUNZE, G. (1954*a*). *N. Jb. Min. Mh.* p. 95.

JAGODZINSKI, H. & KUNZE, G. (1954*b*). *N. Jb. Min. Mh.* p. 113.

JAGODZINSKI, H. & KUNZE, G. (1954*c*). *N. Jb. Min. Mh.* p. 137.

JAHNKE, E. & EMDE, F. (1952). *Tables of Higher Functions*, 5th ed. Leipzig: Teubner.

WHITTAKER, E. J. W. (1953). *Acta Cryst.* **6**, 747.

WHITTAKER, E. J. W. (1954). *Acta Cryst.* **7**, 827.

Acta Cryst. (1955). **8**, 265

The Diffraction of X-rays by a Cylindrical Lattice. III

BY E. J. W. WHITTAKER

Ferodo Limited, Chapel-en-le-Frith, Stockport, England

(*Received* 30 *November* 1954)

Previous papers in this series have dealt with the mathematical theory of diffraction by circular cylindrical lattices. The results have now been confirmed by model optical diffraction experiments, and this method has been used to investigate diffraction by spiral cylindrical lattices and incomplete circular cylindrical lattices.

1. Introduction

In Parts I and II of this series (Whittaker, 1954, 1955) the concept of a cylindrical lattice has been defined, and the diffraction of X-rays by a circular cylindrical lattice has been investigated mathematically on account of its relevance to diffraction by chrysotile fibres and other related minerals. In Part I it was, however, pointed out that a cylindrically curved layer structure might well be expected to adopt a spiral form rather than the form of a set of coaxial circular cylinders. The mathematical theory for diffraction by a spiral cylindrical lattice was at that time still being investigated. However, this has proved intractable and recourse has therefore been taken to the technique of optical diffraction developed by Hanson, Lipson & Taylor (1953) to study the effect in this case. The theory of the importance of spiral cylindrical structures has been more fully developed independently by Jagodzinski & Kunze (1954), who have also proposed an approximate mathematical approach, but the experimental approach described here seems to be more fruitful. In order to facilitate comparison between the diffraction effects from spiral and circular cylindrical lattices, the latter have also been studied in the same way, and the results have confirmed the conclusions already reached in Parts I and II. Since in an actual fibrous specimen it must be anticipated that there will be present broken fibres and incomplete cylindrical layers, the diffraction effects from such structures are also of interest and have been investigated at the same time.

The optical diffraction apparatus developed by Hanson, Lipson & Taylor does not permit the study of diffraction patterns from three-dimensional objects, and it has therefore been necessary to investigate only the diffraction from plane circular and spiral lattices. However, this does not involve any serious limitation, since the diffraction pattern obtained from such a lattice is equivalent to the distribution of intensity on the zero-layer plane in reciprocal space for the corresponding cylindrical lattice. Moreover, we have already shown that, for a structure in which all the scattering matter is concentrated at the lattice points, the distribution of intensity in the diffuse reflexions is identical on all such layer planes, and it is also identical in the sharp reflexions if $\beta = \frac{1}{2}\pi$.

The optical transforms obtained are described in the logical order of increasing complexity, namely the transforms of circular, incomplete circular, and spiral arrays, and under each of these headings the transform of a single element of the array (single circle, spiral turn etc.) is considered before the complete lattice. Finally, comparisons are made in terms which are relevant to the interpretation of X-ray diffraction by fibres.

2. Experimental

The diffraction apparatus used was the actual apparatus described by Hughes & Taylor (1953). The pinhole source used was 10 microns in diameter in order to obtain the highest possible resolution. The masks were prepared with the pantograph punch to a scale of 0·321 mm./Å and each lattice point was represented by a hole 0·5 mm. in diameter. Examples are shown in Fig. 1. Most of the lattices studied had a and b dimensions corresponding to those of the cell of chryso-

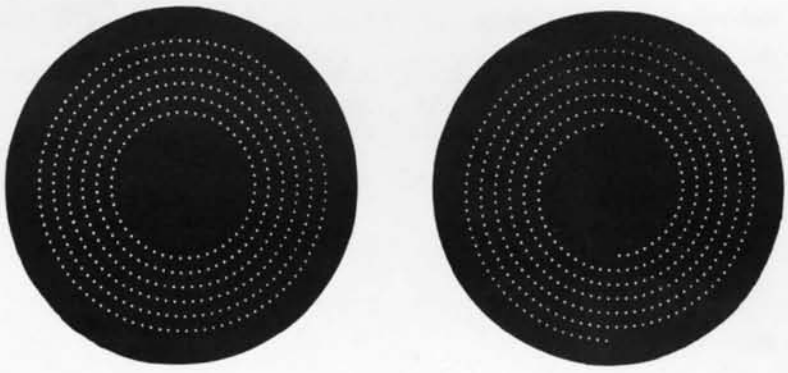

(*a*) (*b*)

Fig. 1. Mask for (*a*) circular lattice, (*b*) double spiral lattice.

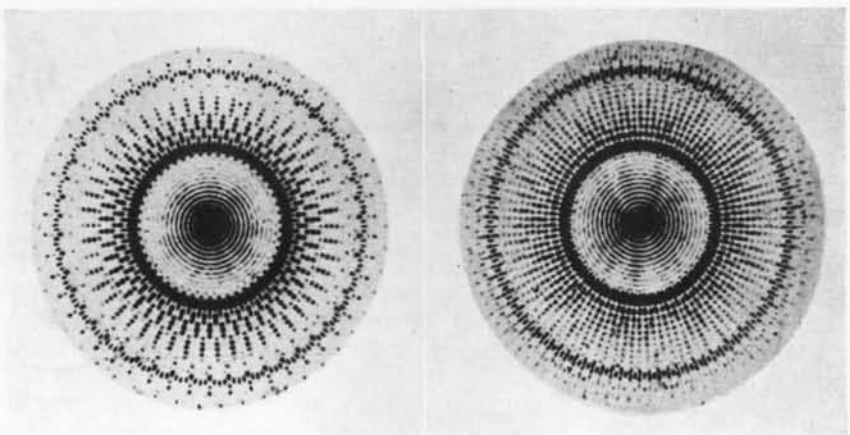

(*a*) (*b*)

Fig. 2. (*a*) Transform of 50 points equally spaced round a circle (innermost circle of Fig. 1(*a*)).
(*b*) Transform of 49 points equally spaced round a circle.

tile in the projection down the *c* axis, i.e. $a = 7{\cdot}3$ Å, $b = 4{\cdot}6$ Å. These are each half of the true *a* and *b* dimensions of chrysotile on account of the halving of the cell in this projection. In order to elucidate some particular points, a few lattices with other axial dimensions were also studied. The drawings from which the masks were prepared were constructed on a scale twelve times as great by the following method. The loci of the lattice points were drawn first. In the case of the spirals this was done by plotting the curve from the equation in polar coordinates. The lattice points were then set off at equal distances with dividers, their positions being checked and corrected from arc-length calculations at least every 90°. The optical transforms were photographed directly on fine-grain film and enlarged on a Vickers projection microscope.

It has been pointed out in II that in an X-ray rotation photograph of a cylindrical lattice the intensity distribution observed is that given by

$$\xi LI(\xi, l) = \frac{\xi L}{2\pi}\int_0^{2\pi} |F(\xi, \Upsilon, l)|^2 d\Upsilon .$$

In order to facilitate comparison between the results of the optical diffraction experiments and the X-ray results it is therefore desirable to perform this integration optically. This has been achieved by rotating the mask continuously in the optical diffraction apparatus during the photography of the transform. A large ball race, with internal diameter greater than that of the lattice punched in the mask, was mounted on the stage of the apparatus; a pulley with a central hole of the same size was mounted directly on the inner race, and the mask was mounted on the pulley. A slow rotation could then be applied to the mask via the pulley. Neither accurate centring of the mask nor uniformity of motion was required in order to give a satisfactory result, which is conveniently described as a rotated transform. An example is shown in Fig. 7(*b*).

The first zero of the diffraction pattern from a single hole of the size used in this work occurs (on the scale adopted) at $\xi/\lambda = 0{\cdot}78$ Å^{-1}, but the transforms obtained are useful only in the range $\xi/\lambda < 0{\cdot}5$ Å^{-1}, which is approximately the radius to which they are reproduced in the plates.

3. An array of points on a circle

The theory in this case has previously been given by Fock & Kolpinsky (1940), and the diffracted amplitude may be written conveniently in the alternative forms:

$$F(\xi, \Upsilon) = pJ_0\left(\frac{2\pi}{\lambda}a_0\xi\right) + 2p\sum_{K=1}^{\infty} i^{Kp}J_{Kp}\left(\frac{pb}{\lambda}\xi\right)\cos Kp(\Upsilon-\varepsilon)$$

$$= pJ_0(pk)+2p\sum_{K=1}^{\infty} i^{Kp}J_{Kp}(pk)\cos Kp(\Upsilon-\varepsilon), \quad (1)$$

where the symbols have the meanings defined in I and II, and constant factors are omitted. The optical transforms for two cases with $a_0 = 36{\cdot}5$ Å, $p = 50$, and $a_0 = 35{\cdot}8$ Å, $p = 49$, are shown in Fig. 2(*a*) and Fig. 2(*b*) respectively. The transforms each contain three conveniently distinguished regions, namely $0<\xi/\lambda<0{\cdot}2$ Å^{-1}, $0{\cdot}2<\xi/\lambda<0{\cdot}4$ Å^{-1}, and $\xi/\lambda>0{\cdot}4$ Å^{-1}.

In the first of these regions $J_p(pk)$ and all Bessel functions of higher order are sensibly zero, and the pattern consists of a series of circular fringes of decreasing intensity corresponding to the term $J_0^2\left(\frac{2\pi a_0}{\lambda}\xi\right)$. It will be convenient to call the part of the transform which depends on this term the *h*-pattern; it is the same as the transform of an annular slot.

In the second region the term in $J_p(pk)$ becomes dominant and it will be convenient to call the part of the transform which depends on this term the *k*-pattern. In this region the rings are broken up into $2p$ radial rows of spots corresponding to the $2p$ maxima of the factor $\cos^2 p(\Upsilon-\varepsilon)$. In the case with p even (Fig. 2(*a*)), expression (1) is wholly real and the sign of the term $J_p(pk)\cos p(\Upsilon-\varepsilon)$ alternates from one radial row to the next. Addition of the $J_0(pk)$ term to it therefore leads to quite different intensity distributions along alternate radial rows, in spite of the relatively small amplitude of $J_0(pk)$ in this region. The calculated intensity distributions are shown in Fig. 3(*a*) and may be seen to be in good agreement with Fig. 2(*a*). In the case with p odd (Fig. 2(*b*)), the term in $J_p(pk)$ is wholly imaginary and accordingly the *h*-pattern and the *k*-pattern are unable to interfere: there are therefore $2p$ similar radial rows along each of which the intensity varies as $J_0^2(pk)+4J_p^2(pk)$. The corresponding theoretical intensity curve is shown in Fig. 3(*b*), and the agreement with Fig. 2(*b*) is also good.

In the third region higher-order Bessel functions become successively dominant and the phenomena become correspondingly more complicated. As only a very small portion of this region is accessible to observation, and the phenomena to be expected are not essentially different, it is not considered further.

Photographs of the transforms (not illustrated) of other arrays of points on circles have confirmed, in accordance with the theory, that the fringe spacing in the *h*-pattern is inversely proportional to a_0, that the radius at which the *k*-pattern begins is inversely proportional to b, and that the number of radial rows in the *k*-pattern is proportional to p.

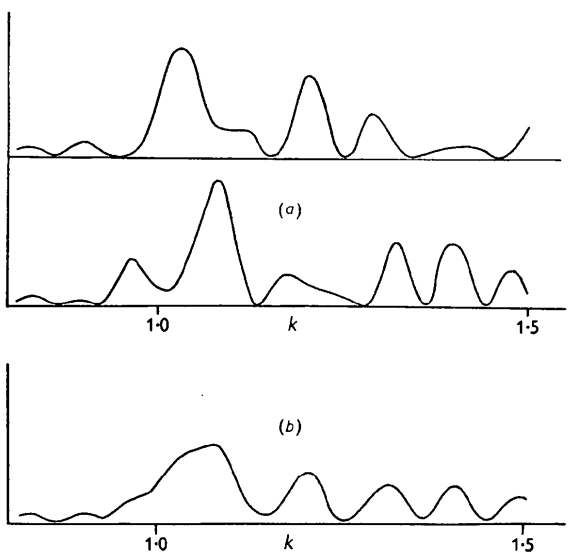

Fig. 3. (*a*) Calculated intensity curves along two adjacent radial rows of spots in the transform of an array of 50 points equally spaced round a circle. The corresponding transform is shown in Fig. 2(*a*).

(*b*) Calculated intensity curve along a radial row of spots in the transform of an array of 49 points equally spaced round a circle. The corresponding transform is shown in Fig. 2(*b*).

4. The circular lattice

The transforms of two types of circular lattices have been studied. In one of these the successive circles are ordered as fully as possible with respect to each other by putting the initial point of each circle on the same radial line (Fig. 4(*a*) and (*b*)). In the other, random displacements are introduced between the initial point of each circle and the radius through the corresponding point of the next smaller circle (Fig. 4(*c*)).

The first three *h*,0 reflexions (corresponding to the *h*0*l* reflexions from a cylindrical lattice) are clearly visible in Fig. 4(*a*) and (*b*) and have the fine structure predicted in I. The rings corresponding to the 1,0 reflexion are continuous, as expected, whereas those corresponding to the 2,0 and 3,0 reflexions are discontinuous. In the case illustrated in Fig. 4(*b*) the number of points on each circle is odd, and accordingly the *h*-pattern and *k*-pattern are $\frac{1}{2}\pi$ out of phase in this region and do not interfere with one another. In this case the discontinuities have been shown to arise from instrumental aberrations. When the number of points is even the two patterns interfere and the discontinuities are much more marked. The tenfold symmetry of the *k*-pattern arises from the relation $2\pi a = 10b$. The sharpness of the maxima as a function of Υ, their fine structure, and their arch-like loci as a function

of ξ, are all to be expected from the superposition of terms like (1) from each of the circles composing the lattice.

Fig. 4(*c*) shows the corresponding transform of a disordered circular lattice with an even number of points on each circle. The tenfold symmetry is still perceptible, but the maxima as a function of Υ are blurred by the disorder. The 2,0 and 3,0 rings are very discontinuous owing to the more marked interference between the *h*- and *k*-patterns in this case, which arises from the greater intensity of the latter at most values of Υ.

5. Incomplete circular arrays

Diffraction by an array of equally spaced points arranged on a circular arc has been investigated theoretically by Blackman (1950) for the case when the number of points on the arc is very large. An analytical solution of the problem for semicircular arcs has also been given by Jagodzinski & Kunze (1954), but no numerical computations from their result have been given. A complete interpretation of the present results has not been sought, but the following features are to be noted:

(i) Fig. 5(*a*) shows the transform of an array of 13 points lying on an arc just larger than a quadrant. Along the direction of the chord of the arc the fringes of the *h*-pattern are 50–75% further out than the corresponding fringes of $J_0^2(pk)$, and fade away rapidly. Also along this direction, the *k*-pattern resembles that from a 50-point circle as far as a value of $k \simeq 1{\cdot}4$, where a cut-off occurs. Both these observations accord at least qualitatively with Blackman's theory. The phenomena remote from this direction are complex and have not been interpreted.

(ii) Fig. 5(*b*) shows the transform of an array of 25

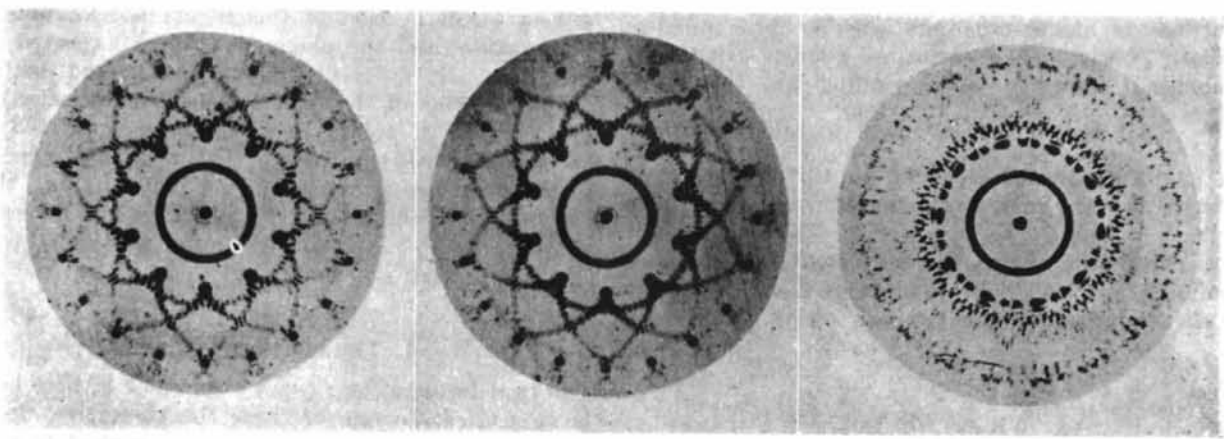

(*a*) (*b*) (*c*)

Fig. 4. (*a*) Transform of ordered circular lattice with an even number of points on each circle (Fig. 1(*a*)).
(*b*) Transform of ordered circular lattice with an odd number of points on each circle.
(*c*) Transform of a disordered circular lattice.

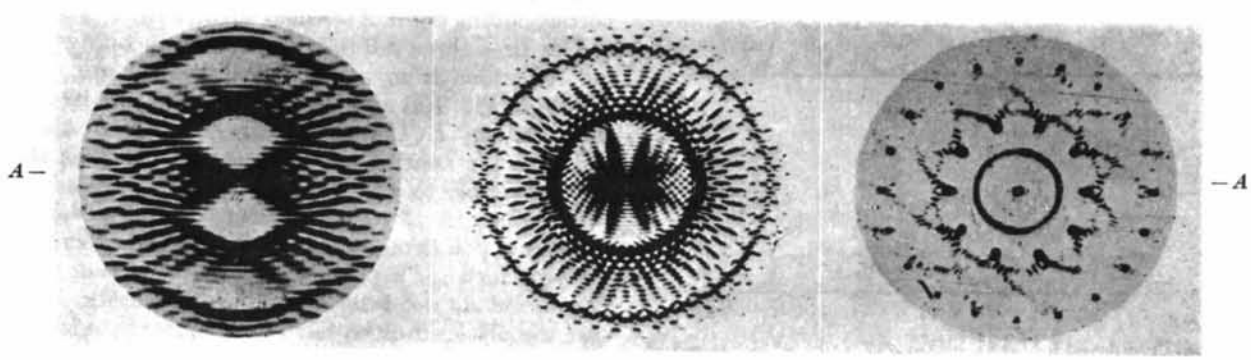

(*a*) (*b*) (*c*)

Fig. 5. (*a*) Transform of 13 points equally spaced on a quadrant of a circle. The line *AA* shows the direction of the bisector of the quadrant.
(*b*) Transform of 25 points equally spaced on a semicircle. The line *AA* shows the direction of the bisector of the semicircle.
(*c*) Transform of a semicircular lattice (half of the lattice used for Fig. 4(*a*)). The line *AA* shows the direction of the bisector of the semicircular lattice.

points lying on a semi-circle. The h-pattern consists of two sets of intersecting hyperbola-like fringes. Perpendicular to the direction of the bisector of the semi-circle the fringes are in the same positions as the maxima of $J_0^2(pk)$. Further reference will be made to these fringes in § 6.

(iii) Fig. 5(c) shows the transform of a semi-circular lattice consisting of half the lattice shown in Fig. 1(a). It closely resembles the transform of the corresponding circular lattice except that all the fine-structure fringes are blurred unless they lie parallel to the bisector of the semi-circles. Also the maxima of the k-pattern vary markedly in intensity round the circle, and the radial discontinuities along the arches of the k-pattern are less regular in position. Further reference will be made to this last point in § 8.

(iv) In the transform of a quadrant lattice these effects are still further intensified. The fine structure disappears in the h-pattern, which only occupies two opposite quadrants. The arch-like loci of the k-pattern are normal but are only partly occupied, and the positions of the discontinuities are still less regular.

6. An array of points on a spiral turn

Because the structure of chrysotile contains two layers in the unit cell, if it has a spiral cylindrical structure that structure must be based on two interleaved spirals. We are therefore primarily interested in figures of this type, which may be conveniently called 'double spirals'. A corresponding mask is illustrated in Fig. 1(b). The portion of this figure which most nearly corresponds to a single circle consists of the first half turn of each arm of the double spiral. Two cases have been investigated: in one the points on the two arms are arranged centrosymmetrically, and in the other they are arranged antisymmetrically about the centre. The transforms of these two arrangements are shown in Fig. 6(a) and (b).

The h-patterns in these two transforms are identical. This is to be expected, since the h-pattern is the transform of the continuous curve on which the points are arranged. It is found that in any particular direction (remote from the discontinuities between the two arms of the spiral) the fringes in the h-pattern lie at the same radii as the fringes in the transform of a circle whose diameter is equal to the diameter of the spiral in that direction. In the direction of the discontinuity between the two arms of the spiral the fringes therefore get out of phase with one another, except in the neighbourhood of integral h values. In these regions the fringes join up to form a $4h$-fold spiral. The corresponding transform of one turn of a single spiral has been shown to behave analogously in giving $2h$-fold spiral fringes in these regions; in the region where the fringes are out of step, however, the phenomena are more complicated as the amplitude is complex. Branching of the fringes occurs and can be explained quantitatively in terms of the same theory.

Superimposed on the above fringe system there is also another system which is identical with the h-pattern of the semicircle transform. It appears probable that this feature arises from the open-ended character

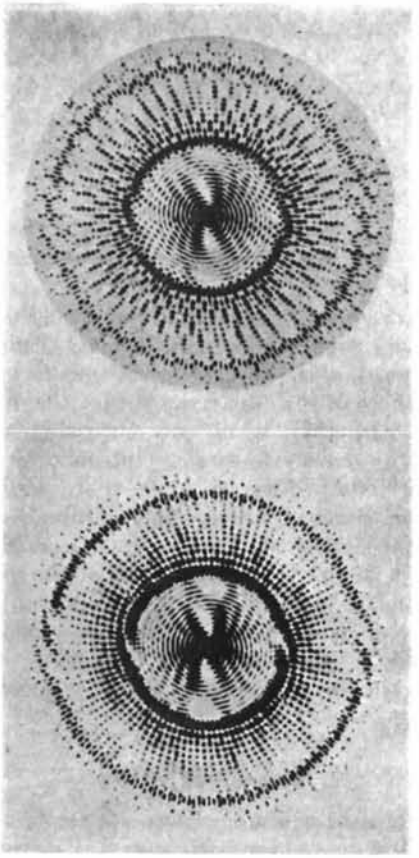

Fig. 6. (a) Transform of equally spaced points arranged symmetrically on two half turns of a double spiral (innermost two half turns of Fig. 1(b)).
(b) Transform of equally spaced points arranged antisymmetrically on two half turns of a double spiral.

of both the semicircle and the two half turns of the double spiral. A similar feature occurs on the transform of the single spiral, but it is much less intense compared with the rest of the transform; this would accord with the above explanation, since the open-ended character is reduced.

The k-patterns of the two transforms (Fig. 6(a) and (b)) differ from one another in the same way as do those of circles containing an odd and even number of points respectively. It is clear that the form of the amplitude of the k-pattern resembles that in the transform of the circular array, and is real or imaginary according to the symmetry of the mask. Clearly in the case of the spiral there arise also intermediate possibilities between centrosymmetry and antisymmetry.

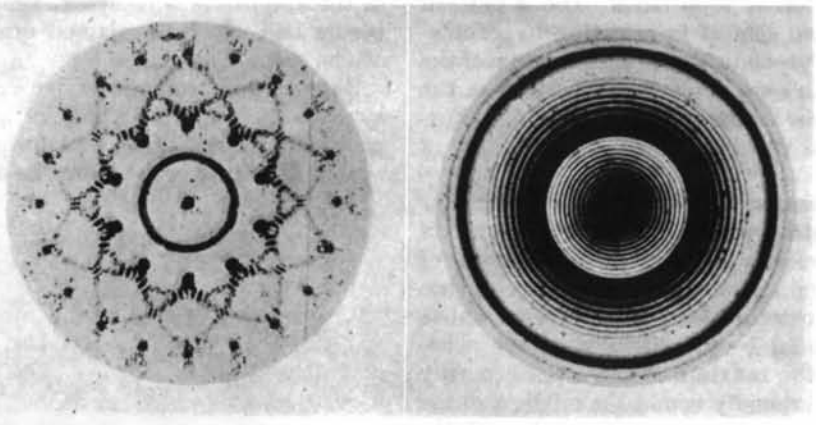

(*a*) (*b*)

Fig. 7. (*a*) Transform of double spiral lattice. (*b*) Rotated transform corresponding to Fig. 2(*a*).

Such cases have not been studied but would obviously lead to more complicated transforms. Although the general features of the k-patterns are thus recognizably related to those of the circle transforms, the details are so complicated that it is not surprising that the mathematical transformation is intractable. Instead of straight radial rows of spots there are slightly curved rows, some of which either bifurcate or unite with an adjacent row as the radius increases. Moreover, these branch points are so disposed that the number of rows remains close to $2p$ over an angular range of 2π. Also, the spots lie on spirals of a rather irregular form which branch into spirals of increasing order in traversing the branch points of the approximately radial rows.

7. The spiral lattice

The transform of a double spiral lattice is shown in Fig. 7(*a*). The resemblance to Fig. 4(*a*) is very striking, and is much closer than that between Figs. 2(*a*) and 6(*a*). The following differences do exist, however:

(i) The h,0 reflexions have a fine structure which consists of a $4h$-fold spiral. The formation of this fine structure can be readily understood. It is due to the summation by amplitude of the fringes of the h-pattern from each successive turn of the spiral lattice. These fringes form a continuous $4h$-fold spiral in the vicinity of the integral values of h, where they will combine to give a ring with the corresponding fine structure; elsewhere they will destructively interfere, just as in the circular case.

(ii) The k-pattern consists of a pattern of arches similar to those on the transform of the circular lattice. However, the symmetry is only approximately tenfold in this case; many of the spots making up the pattern do not lie in exactly the same positions on the various arches, a fact which clearly arises from the spiral character of the k-patterns of the individual turns of the lattice.

8. Rotated transforms

Rotated transforms were recorded, by the method described in § 2, for the various types of array and lattice discussed in §§ 3–7, and an example is illustrated in Fig. 7(*b*). The results obtained may be summarized as follows:

(i) The k-patterns are indistinguishable in the rotated transforms of both odd and even arrays of points on a single circle. This agrees with the theory, according to which the intensity distribution, after integrating over 2π with respect to Υ, is of the form

$$J_0^2(kp)+2J_p^2(kp) \quad \text{for} \quad k < 1{\cdot}9\,.$$

(ii) The k-patterns are also indistinguishable in the rotated transforms of ordered and disordered circular lattices in this region. This also accords with the theory.

(iii) The rotated transforms of the circular lattices are distinguishable from those of the semicircular and spiral transforms by the blurring of the fine structure of the latter in both the h- and k-patterns. This obviously arises ultimately from the distortion of the fringes and spots away from circular loci in the transforms of individual arrays in these lattices.

Since the distinction between spiral and circular lattices is of practical importance in the study of fibrous silicates, the last point has been investigated further. The difference in the h-patterns is of less importance than the difference in the k-patterns; it would be detectable only in diffraction by a single cylindrical lattice and not in diffraction by a specimen in which there were many such lattices of varying diameters, when the fine structure would be obliterated

even if they were circular. On the other hand, the fine structure of the k-pattern, and in particular the deep minimum following the main maximum, would persist to a very large extent under such circumstances. The effect of the spiral and incomplete circular structures on this region of the pattern was therefore investigated further by microdensitometry of the rotated transforms. For this purpose lattices were used in which the value of a was reduced from $5b/\pi$ to $4b/\pi$, in order to avoid overlapping of the 2,0 reflexion on the first minimum of the 0,1 reflexion. The microdensitometer traces are shown in Fig. 8. The progressive diminution

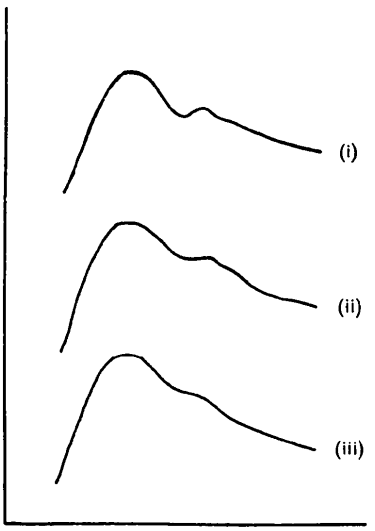

Fig. 8. Micro-densitometer records along radial lines in rotated transforms of (i) a circular lattice, (ii) a spiral lattice, and (iii) a semicircular lattice.

of the first minimum may clearly be correlated with the increasing number of open ends of the lattices studied, namely:

circular lattice:	0,
double spiral lattice:	4,
semicircular lattice:	14.

9. Conclusion

The theory of diffraction by circular cylindrical lattices presented in Parts I and II, only the grosser features of which can be compared with practicable diffraction observations on fibrous minerals, has been confirmed in detail. It has been shown further that structures based on spiral and incomplete circular cylindrical lattices will give diffraction patterns containing both sharp and diffuse reflexions, similar to those given by circular cylindrical lattices. The only feature which is likely to afford a method of distinguishing between these possible types of lattices in fibrous aggregates is the profile of the diffuse reflexions. The application of the results in the determination of the structure of chrysotile will be discussed in a subsequent paper.

I should like to thank Dr H. Lipson for the facilities which he very kindly provided for the use of the optical diffraction apparatus at Manchester College of Technology, and the Directors of Ferodo Ltd for permission to publish this paper.

References

Blackman, M. (1950). *Proc. Phys. Soc.* B, **64**, 631.
Fock, V.A. & Kolpinsky, V.A. (1940). *J.Phys. U.S.S.R.* **3**, 125.
Hanson, A. W., Lipson, H. & Taylor, C. A. (1953). *Proc. Roy. Soc.* A, **218**, 371.
Hughes, W. & Taylor, C. A. (1953). *J. Sci. Instrum.* **30**, 105.
Jagodzinski, H. & Kunze, G. (1954). *N. Jb. Min. Mh.* p. 137.
Whittaker, E. J. W. (1954). *Acta Cryst.* **7**, 827.
Whittaker, E. J. W. (1955). *Acta Cryst.* **8**, 261.